

Synthesis, Cytotoxic Effect, and Structure–Activity Relationship of Pd(II) Complexes with Coumarin Derivatives

Elżbieta Budzisz,^{*,†} Magdalena Małecka,[‡] Ingo-Peter Lorenz,[§] Peter Mayer,[§] Renata A. Kwiecień,^{||} Piotr Paneth,^{||} Urszula Krajewska,[⊥] and Marek Rózalski[⊥]

Departments of Cosmetic Raw Materials Chemistry and Pharmaceutical Biochemistry, Faculty of Pharmacy, Medical University of Łódź, Muszyńskiego 1, 90-151 Łódź, Poland, Department of Crystallography and Crystal Chemistry, University of Łódź, Pomorska 149/153, 90-236 Łódź, Poland, Department of Chemistry and Biochemistry, Ludwig Maximilians University, Butenandtstrasse 5-13 (D), D-81377 Munich, Germany, and Institute of Applied Radiation Chemistry, Department of Chemistry, Technical University of Łódź, Zeromskiego 116, 90-924 Łódź, Poland

Received April 3, 2006

We report the influence of the substituent at the N atom of the ligands on the synthesis, biological activity, and stability of Pd(II) complexes of the general formula PdL₂. The compounds adopt a cis or trans configuration with respect to the substituent at the nitrogen atom. Sterically hindered substituents promote the formation of trans isomers, whereas when the nitrogen atom is unsubstituted, cis isomers are formed. The compounds were characterized by elemental analysis, infrared and ¹H NMR spectroscopies, and electrospray mass spectrometry. The complexes were also studied using X-ray diffraction and computational DFT methods. Both complexes *cis*-**3a** and *trans*-**3c** exhibit square-planar geometries around the Pd(II) atom. The cytotoxic effects of these complexes were examined on two human leukemia cell lines, HL-60 and NALM-6. Pd complex *cis*-**3a** showed significant cytotoxic activity. The effects exhibited by this complex were comparable to those reported for carboplatin. Ligand **2a** was not cytotoxic. Computational analysis carried out at the PB/B3LYP/LACVP**//mPW1PW91/LanL2DZ level showed excellent correlation between the energy difference of the cis and trans isomers and the cytotoxic activity, rendering computations a useful predictive tool for the design of new drugs.

Introduction

Over the past several years, inorganic chemistry has played an important role in modern medicine. The development of metal-based therapeutics has been stimulated by the discovery of cisplatin [*cis*-diamminedichloroplatinum(II), Figure 1a], which is widely used as a drug in chemotherapy,^{1,2} yet

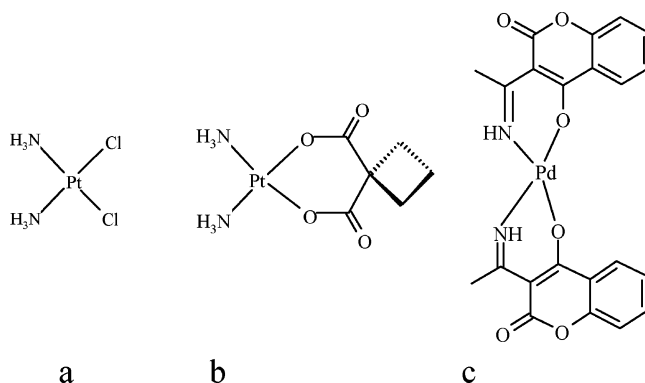


Figure 1. Structures of (a) cisplatin, (b) carboplatin, and (c) Pd(II) complex.

exhibits a wide range of side effects.³ In recent years, investigations have been directed toward searching for new

* To whom correspondence should be addressed: Dr. hab. Elżbieta Budzisz, Department of Cosmetic Raw Materials Chemistry, Faculty of Pharmacy, Medical University of Łódź, 90-151 Łódź, Muszyńskiego 1, Poland. E-mail: elora@ich.pharm.am.lodz.pl.

[†] Department of Cosmetic Raw Materials Chemistry, Faculty of Pharmacy, Medical University of Łódź.

[‡] University of Łódź.

[§] Ludwig Maximilians University.

^{||} Technical University of Łódź.

[⊥] Department of Pharmaceutical Biochemistry, Faculty of Pharmacy, Medical University of Łódź.

(1) Jakupec, M. A.; Galanski, M.; Keppler, B. K. *Rev. Physiol. Biochem. Pharmacol.* **2003**, *146*, 1–53.

(2) Heim, M. E. In *Metal Complexes in Cancer Chemotherapy*; Keppler, B. K., Ed.; VCH: Weinheim, Germany, 1993; p 9.

(3) Daugaard, G.; Abildgaard, C. *Cancer Chemother. Pharmacol.* **1989**, *1*, 25.

antitumor transition metal derivatives with better therapeutic properties than cisplatin. Both platinum and nonplatinum complexes have been screened. Clinical application of the second-generation drug carboplatin [*cis*-diammine(1,1-cyclobutanedicarboxylato)platinum(II), Figure 1b] resulted in a significant decrease in the toxic side effects.⁴ Metal complexes that contain coumarin as a ligand show anticoagulant properties^{5,6} and antitumor activity.^{7,8} In particular, complexes with cerium(III), zirconium(IV), copper(II), zinc(II), bismuth(III), and cadmium(II) exhibit pronounced in vitro cytotoxicity.^{9,10} On the basis of the structural and thermodynamic analogy between platinum(II) and palladium(II) complexes,¹¹ a variety of studies on palladium(II) derivatives as potential anticancer drugs have been carried out.¹² The cytotoxic or antitumor activities of many palladium(II) complexes have been investigated.¹³ As a result, relatively weak ligand binding and a predominant tendency to form trans isomers were found.¹⁴ Only a few examples of *cis* conformers have been reported.¹⁵

In a recent article, we reported the synthesis and biological activity of the complex of 3-(1-aminoethyl)-4-hydroxychromen-2-one with palladium(II) (Figure 1c), where the environment of the Pd atom is similar to that in carboplatin.¹⁶ This complex has a 7800-times higher cytotoxicity than carboplatin. In contrast, the Pd(II) and Pt(II) complexes¹⁷ with 3-(1-aminoethylidene)-2-methoxy-2-oxo-2,3-dihydro-2λ⁵-benzo[e][1,2]-oxaphosphinin-4-one exert effects comparable to those reported for cisplatin and carboplatin. The present report includes five newly prepared palladium(II) complexes of the general formula PdL₂, where L represents unsubstituted or N-alkylated (methyl or benzyl group) coumarin derivatives. Synthetic, structural, and preliminary biological studies were carried out to analyze the structure–activity relationships for systems involving palladium(II) centers. We discuss the influence of substituents at the nitrogen atom and at the C3 position of coumarin on the configurations and their biological activity of the complexes. We also used quantum chemical calculations to evaluate the stabilities of the obtained complexes, as well as their

lipophilicities and electronic density distributions on atoms that participate in coordination.

Experimental Section

Materials and Methods. Bis(benzonitrile)palladium(II) chloride was purchased from Sigma. Solvents used in the syntheses were of reagent grade or better quality and were dried according to standard methods. The melting points were determined using an Electrothermal 1A9100 apparatus and are reported as uncorrected values. The IR spectra were recorded on a Pey-Unicam 200G spectrophotometer in KBr or CsI. The ¹H NMR spectra were recorded using a 300-MHz Varian Mercury spectrometer. The MS data were obtained on an LKB 2091 mass spectrometer (70 eV ionization energy), and the ESMS were recorded on a 5989A mass spectrometer with a 59980B particle-beam LCMS interface (Hewlett-Packard). For the new compounds, satisfactory elemental analyses (±0.4% of the calculated values) were obtained in the Microanalytical Laboratory of the Department of Bioorganic Chemistry (Medical University, Lodz, Poland) using a Perkin-Elmer PE 2400 CHNS analyzer. Ethyl 2-phenyl-4-oxo-4*H*-chromene-3-carboxylate (**1a**), methyl 2-methyl-4-oxo-4*H*-chromene-3-carboxylate (**1b**), 3-(1-methylaminoethyl)-4-hydroxychromen-2-one (**2d**), and 3-(1-benzylaminoethyl)-4-hydroxychromen-2-one (**2e**) were prepared according to literature procedures.^{18,19}

Synthesis of the Ligands. Synthesis of 3-(1-Aminobenzylidene)-2*H*-chromene-2,4(3*H*)-dione (2a). A 25% aqueous ammonia solution (0.31 mL, 2 mmol) in ethanol (0.5 mL) was added at room temperature to a solution of ethyl 2-phenyl-4-oxo-4*H*-chromene-3-carboxylate (**1**) (588.6 mg, 2 mmol) in ethanol (10 mL). After 24 h, the precipitated solid crude product was filtered off, dried, and recrystallized from methanol (10 mL).

Compound **2a** was obtained as a white solid (482.7 mg, 91.0%); mp 236.3–237.4 °C (lit.²⁰ 223–226 °C). ¹H NMR (DMSO-*d*₆): δ 7.22–7.97 (m, 9H, aromatic), 10.12 (s, 1H, OH), 12.00 (s, 1H, NH). ¹³C NMR (DMSO-*d*₆): δ 94.77, 116.02, 120.04, 123.21, 125.91, 126.78, 127.55, 129.57, 133.73, 136.08, 153.10, 160.89, 175.14, 179.17 (C=O). MS *m/z* (%): 266 (100, M⁺). C₁₆H₁₁NO₃ (265.26): calculated C 72.44, H 4.18, N 5.28; found C 72.23, H 3.85, N 5.32%.

General Procedure for Compounds 2b,c. A solution of methyl- or benzylamine (20 mmol) in methanol (1.0 mL) was added at room temperature to a solution of 2-phenyl-4-oxo-4*H*-chromene-3-carboxylic acid ethyl ester (**1a**) (20 mmol) in methanol (5 mL). The solid crude product, which precipitated after several minutes, was filtered off, dried, and recrystallized from methanol. Compounds **2b** and **2c** were obtained as white solids.

3-(1-Methylaminobenzylidene)-2*H*-chromene-2,4(3*H*)-dione (2b). Yield: 480.3 mg, 86.5%; mp 134.5–135.9 °C. ¹H NMR (DMSO-*d*₆): δ 2.85 (s, 3H, N–CH₃) 7.21–7.97 (m, 9H, aromatic), 13.37 (s, 1H, OH). ¹³C NMR (DMSO-*d*₆): δ 32.31 (N–CH₃), 95.89, 116.23, 120.16, 125.43, 128.40, 153.95, 160.35, 174.98, 179.36 (C=O). MS *m/z* (%): 280 (100, M⁺). C₁₇H₁₃NO₃ (279.28): calculated C 73.10, H 4.69, N 5.02%; found C 72.74, H 4.64, N 5.02%.

3-(1-Benzylaminobenzylidene)-2*H*-chromene-2,4(3*H*)-dione (2c). Yield: 494.7 mg, 69.6%; mp 144.2–146.1 °C. ¹H NMR (DMSO-*d*₆): δ 4.41 (d, 2H, N–CH₂Ph), 7.21–7.96 (m, 14H, aromatic), 13.92 (s, 1H, OH). ¹³C NMR (DMSO-*d*₆): δ 48.44 (CH₂), 96.17, 116.25, 123.53, 125.50, 126.06, 127.33, 153.41, 160.45, 179.91

- (4) Shehata, M. R. *Transition Met. Chem.* **2001**, *26*, 198–204.
- (5) Jiang, D.; Deng, R.; Wu, J. *Wuji Huaxue* **1989**, *5*, 21–28.
- (6) Deng, R.; Wu, J.; Long, L. *Bull. Soc. Chim. Belg.* **1992**, *101*, 439–443.
- (7) Kostova, I.; Manolov, I.; Konstantinov, S.; Karaivanova, M. *Eur. J. Med. Chem.* **1999**, *34*, 63–68.
- (8) Manolov, I.; Kostova, I.; Netzeva, T.; Konstantinov, S.; Karaivanova, M. *Arch. Pharm. Pharm. Med. Chem.* **2000**, *333*, 93–98.
- (9) Kostova, I.; Malonov, I.; Karaivanova, M. *Archiv. Pharm. Pharm. Med. Chem.* **2001**, *334*, 157–162.
- (10) Karaivanova, V. D.; Malonov, I.; Minassyan, M. L.; Danchev, N. D.; Samurova, S. M. *Pharmazie* **1994**, *49*, 856–857.
- (11) Rau, T.; van Eldik, R. In *Metal Ions in Biological Systems*; Sigel, A., Sigel, H., Eds.; Marcel Dekker: New York, 1996; Vol. 32, p 339.
- (12) Al-Allaf, T. A.; Rashan, L. J. *Boll. Chim. Farmac.* **2001**, *140*, 205–210.
- (13) Kuduk-Jaworska, J.; Puzsko, A.; Kubiak, M.; Pelczynska, M. *J. Inorg. Biochem.* **2004**, *98*, 1447–1456.
- (14) Acquaye, J. H. K. A.; Richardson, M. F. *Inorg. Chim. Acta* **1992**, *201*, 101–107.
- (15) Petit, L. D.; Bezer, M. *Coord. Chem. Rev.* **1985**, *61*, 97–114.
- (16) Budzisz, E.; Keppler, B. K.; Giester, G.; Woźniczka, M.; Kufelnicki, A.; Nawrot, B. *Eur. J. Inorg. Chem.* **2004**, 4412–4419.
- (17) Budzisz, E.; Krajewska, U.; Rozalski, M. *Pol. J. Pharmacol.* **2004**, *56*, 473–478.

- (18) Coppola, G. M.; Dodsworth, R. W. *Synthesis* **1981**, *7*, 523–524.
- (19) Budzisz, E.; Brzezinska, E.; Krajewska, U.; Rozalski, M. *Eur. J. Med. Chem.* **2003**, *38*, 597–603.
- (20) Kloss, R. A.; Wiener, C. J. *J. Org. Chem.* **1963**, *28*, 1671–1673.

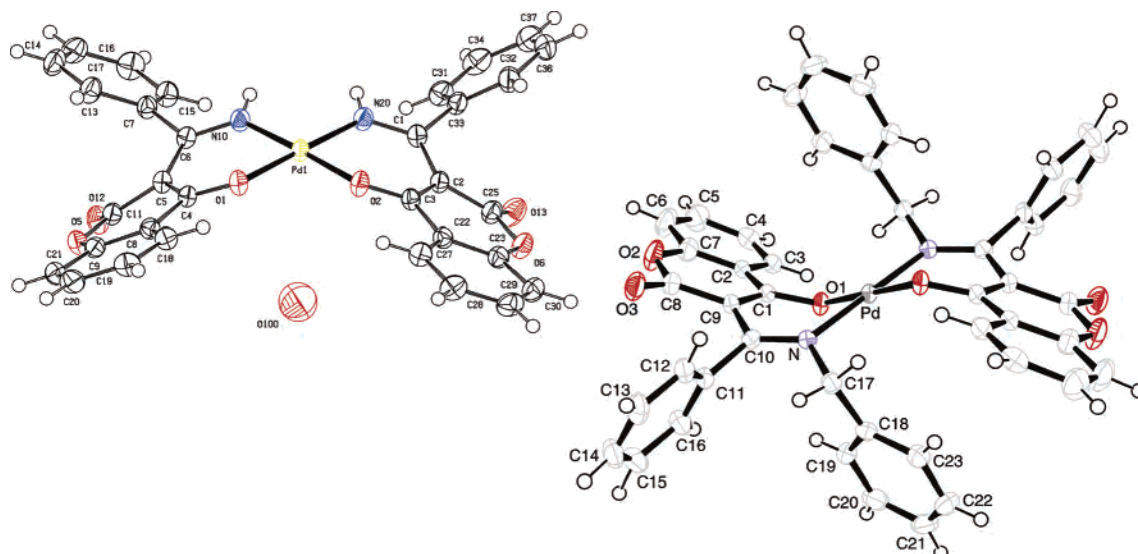


Figure 2. Single-crystal X-ray structures with the atom-numbering schemes of **3a** and **3c**. Displacement ellipsoids are drawn at the 30% probability level.

(C=O). MS m/z (%): 355 (100, M^+). $C_{23}H_{17}NO_3$ (355.37): calculated C 77.73, H 4.82, N 3.94%; found C 77.67, H 4.71, N 3.98%.

General Procedure for Compounds 3a–e. A methanolic solution of **2** (0.5 mmol, in 15 mL of MeOH) was added to a solution of $[Pd(C_6H_5CN)_2Cl_2]$ (95.9 mg, 0.25 mmol) in chloroform/methanol (1:1, v/v, 6 mL). The mixture was stirred at room temperature for 24 h, after which time the resulting yellow crystals were filtered off, washed with water and diethyl ether, and dried overnight in a vacuum over anhydrous silica gel.

Compound 3a. Yield: 103.5 mg (65%); mp >360 °C dec. 1H NMR (DMSO- d_6): δ 7.20–7.96 (m, 18H, aromatic), 12.4 (S_{broad} , 2H, NH). ESMS m/z : 637. $C_{32}H_{20}N_2O_6Pd$ (636.93): calculated C 60.53, H 3.17, N 4.41%; found C 60.67, H 2.91, N 4.48%.

Compound 3b. Yield: 121.5 mg (73.3%); mp 263.5–264.8 °C. 1H NMR (DMSO- d_6): δ 2.84 (2 \times s, 6H, N- CH_3), 7.20–7.96 (m, 18H, arom.). ESMS m/z : 662. $C_{34}H_{24}N_2O_6Pd \cdot 1.5 H_2O$ (689.99): calculated C 59.18, H 3.94, N 4.06%; found C 59.04, H 3.59, N 4.13%.

Compound 3c. Yield: 138.8 mg (68.1%); mp 245.1–245.3 °C. 1H NMR (DMSO- d_6): δ 4.54 (d, 4H, N- CH_2Ph), 7.22–8.14 (m, 18H, aromatic). ESMS m/z : 815. $C_{46}H_{32}N_2O_6Pd$ (815.06): calculated C 67.77, H 3.96, N 3.44%; found C 67.68, H 3.75, N 3.48%.

Compound 3d. Yield: 101.0 mg (75%); mp 261.2–263.0 °C. 1H NMR (DMSO- d_6): δ 2.64 (2 \times s, 6H, C- CH_3), 2.95 (2 \times s, 6H, N- CH_3), 7.29–8.16 (m, 8H, aromatic). ESMS m/z : 538. $C_{24}H_{20}N_2O_6Pd \cdot 0.5 H_2O$ (547.84): calculated C 52.61, H 3.83, N 5.11%; found C 52.58, H 3.93, N 5.11%.

Compound 3e. Yield: 110.4 mg (64%); mp 228.1–229.3 °C. 1H NMR (DMSO- d_6): δ 2.58 (2 \times s, 6H, C- CH_3), 4.43 (d, 4H, N- CH_2Ph), 7.18–8.10 (m, 18H, aromatic). ESMS m/z : 691. $C_{36}H_{28}N_2O_6Pd$ (691.02): calculated C 62.56, H 4.08, N 4.06%; found C 62.48, H 3.75, N 3.96%.

Crystallographic Analysis of Palladium(II) Complexes. Single crystals of compound **3a** were obtained by slow evaporation of a solution of **3a** in chloroform/methanol. Data for a yellow crystal of size 0.4 \times 0.05 \times 0.05 mm were measured at 150 K on a STOE IPDS diffractometer. The unit cell parameters were determined from 36223 reflections in the θ range 1.65–29.33°. 33994 intensities were collected using graphite-monochromatized Mo $K\alpha$ radiation in θ range 1.65–29.39°. 6994 independent reflections were measured in the range $-17 \leq h \leq 17$, $-10 \leq k \leq 10$, $-37 \leq l \leq$

38 [$R(int) = 0.0400$], of which 5898 were observed with $I > 2\sigma(I)$. In the data reduction step, intensities were corrected for Lorentz and polarization effects but not for absorption.²¹ Structures were solved by direct methods using the SHELXS86²² program and refined by full-matrix least-squares calculations on F^2 using SHELXL97.²³ After the refinement with isotropic displacement parameters, the refinement was continued with anisotropic displacement parameters for all non-hydrogen atoms. Positions of all H atoms attached to phenyl groups were determined geometrically and refined using a riding model with $U_{iso}(H) = -1.2U_{eq}(C)$, where the C–H distance was fixed at 0.93 Å. Positions of H atoms for NH groups were found on a Fourier map and refined isotropically.

The final refinement gave $R1 = 0.0264$, $wR2 = 0.0646$, and $S = 1.029$ for the observed reflections. The maximum peak on the final ΔF map was 0.351 $e/\text{Å}^3$, and the minimum was $-0.789 e/\text{Å}^3$. The molecular geometry was calculated using PLATON.²⁴ The drawings were generated using PLATON and are presented in Figure 2. The crystal data and X-ray details are given in the Supporting Information, and the geometric parameters are reported in Table 2 below. Further experimental details have been deposited at the Cambridge Crystallographic Data Centre, CCDC 297227.

Single crystals of compound **3c** were obtained by slow evaporation of a chloroform/methanol solution of **3c**. The data were collected on a Nonius Kappa CCD instrument equipped with a rotating anode generator (Mo $K\alpha$ radiation). The structure was solved with SHELXL97²⁵ using direct methods and refined with SHELXL-97. All non-hydrogen atoms were refined anisotropically; the hydrogen atoms were located in the Fourier map and refined without any restraints. The drawings were generated using PLATON and are shown in Figure 2a. Crystallographic data for **3c** have been deposited with the Cambridge Crystallographic Data Centre as CCDC 299066. Copies of the data can be obtained free of charge

(21) *Software for IPDS-II*; Stoe and Cie: Darmstadt, Germany, 2000.

(22) Sheldrick, G. M. *SHELXS86: Program for Crystal Structure Solution*; University of Göttingen: Göttingen, Germany, 1986.

(23) Sheldrick, G. M. *SHELXL97: Programs for Crystal Structure Analysis*; University of Göttingen: Göttingen, Germany, 1997.

(24) Spek, A. L. *PLATON—Molecular Geometry Program*; University of Utrecht: Utrecht, The Netherlands, 1998.

(25) Altomare, A.; Burla, M. C.; Camalli, M.; Casciaro, G. L.; Giacovazzo, C.; Guagliardi, A.; Moliterni, A. G. G.; Polidori, G.; Spagna, R. *J. Appl. Crystallogr.* **1999**, *32*, 115–119.

Pd(II) Complexes with Coumarin Derivatives

upon application to the CCDC, 12 Union Road, Cambridge CB2 1EZ, U.K. E-mail: deposit@ccdc.cam.ac.uk.

Cell and Cytotoxicity Assay. The cytotoxicity was determined on two human leukemia cell lines, promyelocytic HL-60 and lymphoblastic NALM-6. The NALM-6 cell line was purchased from the German Collection of Microorganisms and Cell Cultures. Cells were cultured in an RPMI 1640 medium supplemented with 10% fetal calf serum in a 5% CO₂/95% air atmosphere. Exponentially growing cells were seeded at 3 × 10⁵ per well of 24-well plate (Nunc), and cells were then exposed to the tested compounds for 48 h. Stock solutions were freshly prepared in DMSO, and then dilutions from 10⁻³ to 10⁻⁷ M in complete culture medium were made.

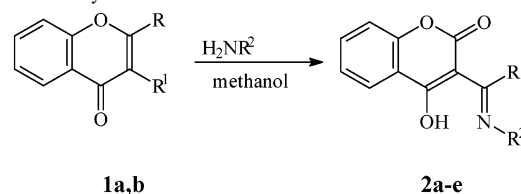
The number of viable cells was counted in a Bürker hemocytometer using the trypan-blue exclusion assay. The values of IC₅₀ (the concentration of test compounds required to reduce the cell survival fraction to 50% of the control) were calculated from dose-response curves and used as a measure of cellular sensitivity to a given treatment. All data are expressed as mean ± standard deviation.

Computational Details. All gas-phase geometry optimizations were performed with the Gaussian 03 package²⁶ using the mPW1PW91 functional²⁷ in the ECP LanL2DZ basis set.^{28,29} Optimization of the *cis*-**3a** structure was also carried out using the family of PMx semiempirical Hamiltonians (PM3-d,³⁰ PM5,³¹ PM6³²) as implemented in the Mopac2002 program.³³ log *P* values were obtained from the free Gibbs energy in water and 1-octanol. Solvation effects of the structures optimized at the mPW1PW91/LanL2DZ level were calculated by the Poisson-Boltzmann (PB) method as implemented in the Jaguar v.6.0 program.³⁴ These energy calculations were carried out at the B3LYP theory level using the LACVP** basis set for palladium and the 6-31G(d,p) basis set for the other atoms. For 1-octanol, the dielectric constant of 10.3 and the solvent probe molecule radius of 3.14 were used. All calculations were carried out using default convergence criteria.

Results

Chemistry. Derivative **2a** was first synthesized by Kloss³⁵ via the reaction of 3-benzoylo-4-hydroxycoumarin with ammonium acetate. We have synthesized ligands **2a–e**

Scheme 1. Synthesis of Coumarin Derivatives **2a–e**



1a R=Ph, R¹=COOC₂H₅

1b R=CH₃, R¹=COOCH₃

2a R=Ph, R²=H

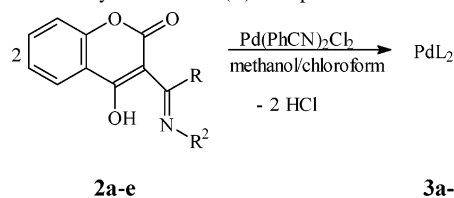
2b R=Ph, R²=CH₃

2c R=Ph, R²=CH₂Ph

2d R=CH₃, R²=CH₃

2e R=CH₃, R²=CH₂Ph

Scheme 2. Synthesis of Pd(II) Complexes **3a–e**



3a R=Ph, R²=H

3b R=Ph, R²=CH₃

3c R=Ph, R²=CH₂Ph

3d R=CH₃, R²=CH₃

3e R=CH₃, R²=CH₂Ph

according to our published methods,²⁰ using the reaction of 2-phenyl-4-oxo-4*H*-chromene-3-carboxylic acid ethyl ester (**1a**) and 2-methyl-4-oxo-4*H*-chromene-3-carboxylic acid methyl ester (**1b**) with primary amines. The compounds were obtained in excellent yields (70–95%). The structures of compounds **2a–e** (Scheme 1) were confirmed by elemental and spectral (IR, ¹H, ¹³C NMR, MS) analyses (see Experimental Section).

Synthesis and Spectral Characteristics of Pd(II) Complexes. The palladium(II) complexes of coumarin ligands (**2a–e**) were synthesized by the addition of a methanol solution of **2a–e** to a chloroform/methanol solution (1:1) of bis(benzonitrile)dichloropalladium(II) in a 1:2 molar ratio. The reaction was carried out at room temperature for 24 h (Scheme 2). The compositions and structures of the resulting complexes **3a–e** were confirmed by elemental analysis, IR spectroscopy, ES mass spectrometry, and X-ray diffraction.

The structures were also confirmed by ¹H NMR analysis of the samples dissolved in DMSO-*d*₆. DMSO was selected as the solvent because of the very limited solubility of all complexes in other solvents. Some characteristic IR spectral data for the complexes **3a–e** and ligands **2a–e** are reported in Table 1.

Significant differences in the IR spectra of complexes **3a–e** were observed in comparison with the spectra of ligands **2a–e**, predominantly in the valency vibrations of the NH group. The ν_{NH} band shifted toward higher frequen-

- (26) Frisch, M. J.; Trucks, G. W.; Schlegel, H. B.; Scuseria, G. E.; Robb, M. A.; Cheeseman, J. R.; Montgomery, J. A., Jr.; Vreven, T.; Kudin, K. N.; Burant, J. C.; Millam, J. M.; Iyengar, S. S.; Tomasi, J.; Barone, V.; Mennucci, B.; Cossi, M.; Scalmani, G.; Rega, N.; Petersson, G. A.; Nakatsuji, H.; Hada, M.; Ehara, M.; Toyota, K.; Fukuda, R.; Hasegawa, J.; Ishida, M.; Nakajima, T.; Honda, Y.; Kitao, O.; Nakai, H.; Klene, M.; Li, X.; Knox, J. E.; Hratchian, H. P.; Cross, J. B.; Bakken, V.; Adamo, C.; Jaramillo, J.; Gomperts, R.; Stratmann, R. E.; Yazyev, O.; Austin, A. J.; Cammi, R.; Pomelli, C.; Ochterski, J. W.; Ayala, P. Y.; Morokuma, K.; Voth, G. A.; Salvador, P.; Dannenberg, J. J.; Zakrzewski, V. G.; Dapprich, S.; Daniels, A. D.; Strain, M. C.; Farkas, O.; Malick, D. K.; Rabuck, A. D.; Raghavachari, K.; Foresman, J. B.; Ortiz, J. V.; Cui, Q.; Baboul, A. G.; Clifford, S.; Cioslowski, J.; Stefanov, B. B.; Liu, G.; Liashenko, A.; Piskorz, P.; Komaromi, I.; Martin, R. L.; Fox, D. J.; Keith, T.; Al-Laham, M. A.; Peng, C. Y.; Nanayakkara, A.; Challacombe, M.; Gill, P. M. W.; Johnson, B.; Chen, W.; Wong, M. W.; Gonzalez, C.; Pople, J. A. *Gaussian 03*, revision D01; Gaussian, Inc.: Pittsburgh, PA, 2003.
- (27) Adamo, C.; Barone, V. *J. Chem. Phys.* **1998**, *108*, 664–675.
- (28) Hay, P. J.; Wadt, W. R. *J. Chem. Phys.* **1985**, *82*, 270–283.
- (29) Wadt, W. R.; Hay, P. J. *J. Chem. Phys.* **1985**, *82*, 284–298.
- (30) Lopez, X.; York, D. M. *Theor. Chem. Acc.* **2003**, 109–148.
- (31) Stewart, J. J. P. Fujitsu Limited, Tokyo, Japan, MOPAC 2002.
- (32) Stewart, J. J. P. Fujitsu Limited, Tokyo, Japan. Personal communication, MOPAC 2002.
- (33) Fujitsu Limited, Tokyo, Japan, MOPAC 2002.
- (34) *Jaguar*, version 6.0; Schrodinger, LLC: New York, 2005.
- (35) See ref 20.

Table 1. Selected IR Bands for Ligands **2a–e** and Complexes **3a–e**

| ν (cm ⁻¹) | NH | —C=O | —N=C— | M—N— | M—O |
|---------------------------|------|------|-------|------|-----|
| 2a | 3238 | 1685 | 1607 | — | — |
| 3a | 3329 | 1709 | 1600 | 446 | 506 |
| 2b | 3458 | 1711 | 1606 | — | — |
| 3b | — | 1708 | 1600 | 443 | 512 |
| 2c | 3448 | 1710 | 1588 | — | — |
| 3c | — | 1721 | 1601 | 460 | 520 |
| 2d | 3393 | 1701 | 1607 | — | — |
| 3d | — | 1701 | 1607 | 459 | 527 |
| 2e | 3382 | 1698 | 1613 | — | — |
| 3e | — | 1701 | 1615 | 461 | 524 |

Table 2. Selected Geometric Parameters of **3a** and **3c** ($i = 2 - x, -y, 2 - z$)

| <i>cis</i> -PdL ₂ (3a) | | <i>trans</i> -PdL ₂ (3c) | |
|--|-----------|--|------------|
| Bond Lengths (Å) | | | |
| O(1)—Pd(1) | 2.012(1) | O(1)—Pd(1) | 1.990(2) |
| N(20)—Pd(1) | 1.961(2) | N(1)—Pd(1) | 2.022(2) |
| O(2)—Pd(1) | 1.999(1) | O(1) ^{<i>i</i>} —Pd(1) | 1.990(2) |
| N(10)—Pd(1) | 1.962(2) | N(1) ^{<i>j</i>} —Pd(1) | 2.022(2) |
| Bond Angles (deg) | | | |
| O(2)—Pd(1)—O(1) | 87.43(5) | O1—Pd—O1 ^{<i>i</i>} | 179.999(1) |
| N(20)—Pd(1)—N(10) | 91.78(7) | N ^{<i>i</i>} —Pd—N | 179.999(1) |
| N(20)—Pd(1)—O(1) | 177.41(6) | O1—Pd—N | 87.87(9) |
| N(10)—Pd(1)—O(2) | 177.77(6) | O1—Pd—N ^{<i>i</i>} | 92.13(9) |
| Torsion Angles (deg) | | | |
| Pd(1)—O(1)—C(4)—C(5) | -12.0(2) | Pd1—O1—C1—C9 | 36.2(2) |
| Pd(1)—N(10)—C(6)—C(5) | 2.9(3) | Pd1—N—C10—C9 | -0.1(2) |
| Pd(1)—O(2)—C(3)—C(2) | 18.8(2) | | |
| Pd(1)—N(20)—C(1)—C(2) | -1.6(3) | | |

cies: from 3238 cm⁻¹ for compound **2a** to 3329 cm⁻¹ for complex **3a**. For the other complexes, this band disappeared. This observation can be explained by the participation of the nitrogen atom in the coordination with the metal ions in **3a** complexes. The N—Pd band peaks were observed at ~443–461 cm⁻¹ for complexes **3a–e**. Within the range between 600 and 500 cm⁻¹, the bands for the of O—Pd group were observed at ~506 cm⁻¹ for complex **3a** and 520 cm⁻¹ for complex **3c**.

In the ¹H NMR spectra of the complexes, one of the exchangeable protons (at 10.12 ppm), attributed to the OH enol group of **2a**, was not present in the complex, and the NH signal was observed at 12.4 ppm.

Electrospray mass spectrometry (ESMS) is considered one of the most powerful analytical techniques in the field of coordination compounds.³⁶ The spectra obtained by ESMS analysis can show patterns that correspond to [M + H]⁺, [2M + H]⁺, or adducts with solvent molecules.³⁷ ESMS analyses were performed for all complexes in positive-ion mode. ESMS analysis for complex **3a** showed the expected isotope pattern ion at $m/z = 538$.

X-ray Structure. Single-crystal X-ray crystal studies of compound **3a** were undertaken to elucidate the coordination sphere of the palladium(II) center. The molecular structures of the palladium(II) complexes with the atomic numbering scheme are shown in Figure 2, and selected bond lengths and angles are reported in Table 2. In addition to the complex, there one-half molecule of water in the unit cell. The environments of the Pd(II) atom are square-planar,

(36) Plattner, D. A. *Int. J. Mass Spectrom.* **2001**, *207*, 125–144.(37) Henderson, W.; Evans, C. *Inorg. Chim. Acta* **1999**, *294*, 183–192.**Table 3.** Hydrogen Bonding Geometry (Å, deg)

| | D—H | H···A | D···A | D—H···A |
|-----------------------------------|---------|---------|----------|---------|
| N20—H20···O12 ^{<i>i</i>} | 0.77(3) | 2.25(1) | 2.976(2) | 157(1) |
| N10—H10···O12 ^{<i>i</i>} | 0.78(3) | 2.32(1) | 3.065(2) | 159(1) |

formed by two N atoms and two O atoms, and the PdN₂O₂ square adopts a cis configuration. The corresponding Pd—N and Pd—O bond distances (Table 2) are almost equal, whereas the Pd—O distances are 2.0012(2) and 1.999(2) Å and are therefore shorter than the literature values.³⁸ The geometry about the Pd atom deviates little from an ideal square plane; the O(2)—Pd(1)—O(1) angle is slightly smaller than 90°. As a consequence, the corresponding N(20)—Pd(1)—N(10) angle is slightly larger than 90°.

The Pd atom is almost exactly coplanar with the plane defined by the four atoms bonded to it, with a deviation from the “best” plane of -0.0023(1) Å. Ligand 3-(1-aminobenzylidene)-2*H*-chromene-2,4(3*H*)-dione (**2a**) connected to the central Pd atom forms two six-membered rings, which have conformation between boat and twisted-boat. The puckering parameters³⁹ are $Q_T = 0.369(2)$ Å, $\varphi_2 = 14.7(3)^\circ$, $\theta_2 = 71.8(3)^\circ$, $Q_T = 0.360(2)$ Å, $\varphi_2 = -171.8(3)^\circ$, and $\theta_2 = 105.1(3)^\circ$, corresponding to the Pd1, O2, C3, C2, C1, N20 and Pd1, O1, C4, C5, C6, N10 atom sequences, respectively. According to Nardelli,⁴⁰ the asymmetry parameters are $\Delta_2 = 0.048(1)$ and $\Delta_2 = 0.048(1)$ for two 2-fold pseudo-axes passing through the midpoint of the Pd1—O2 bond and the C3 atom and $\Delta_s = 0.033(1)$ and $\Delta_s = 0.049(1)$ for the mirror plane passing through the Pd1 atom and the midpoint of the O1—C4 bond, corresponding to the atom sequences mentioned above. Bond distances and angles for both molecules are in good agreement with the expected values.⁴¹

An examination of the hydrogen bonds present shows conventional N—H···O interactions. The geometry of the hydrogen bond present is presented in Table 3.

Compound **3c** crystallizes in space group $P2_1/n$ with two formula units per unit cell. In the centrosymmetric complex, the Pd(II) is bound by two chelating ligands, resulting in a square-planar coordination sphere. As a consequence of the inversion symmetry, the Pd—N2—O2 core exhibits a trans configuration. The Pd—O1 bond distance is 1.990(2) Å and is slightly shorter than the Pd—N bond distance at 2.022(2) Å. The O—Pd—N1 angle is 87.87(9)°, resulting in a small deviation from an ideal square plane. The chelate formation leads to a six-membered ring Pd—O1—C1—C9—C10—N with the puckering parameters $Q = 0.5969(21)$ Å, $\theta = 110.45(25)^\circ$, and $\varphi = 199.3(3)^\circ$, giving a $B_{1,4}$ boat conformation that is twisted toward ²S₄.

Computational Results. The superior performance of the mPW1PW91/LanL2DZ theory level in comparison with other DFT functionals for the calculation of geometries and vibrations for cisplatin and carboplatin has been docu-

(38) Orpen, A. G.; Brammer, L.; Allen, F. H.; Kennard, O.; Watson, D. G.; Taylor, R. *J. Chem. Soc., Perkin. Trans.* **1987**, *2*, S1–S19.(39) Cremer, D.; Pople, J. A. *J. Am. Chem. Soc.* **1975**, *97*, 1354–1358.(40) Nardelli, M. *J. Appl. Crystallogr.* **1996**, *29*, 296–300.(41) Allen, F. H.; Kennard, O.; Watson, D. G.; Brammer, L.; Orpen, A. G.; Taylor, R. *J. Chem. Soc., Dalton Trans.* **1989**, S1–S83.

Table 4. Selected Geometrical Parameters Obtained for Ligands **2a–2e** from DFT Calculations at the MPW1PW91/LanL2DZ Theory Level

| compd | N–H (Å) | N–H–O (deg) | H–O (Å) |
|-----------|---------|-------------|---------|
| 2a | 1.033 | 135.8 | 1.695 |
| 2b | 1.043 | 141.4 | 1.636 |
| 2c | 1.042 | 140.5 | 1.648 |
| 2d | 1.043 | 142.6 | 1.621 |
| 2e | 1.044 | 141.3 | 1.635 |

Table 5. Values of LogP Calculated from Solvation-Free Energies Obtained at the B3LYP/LACVP**//MPW1PW91/LanL2DZ Theory Level Using the PB Continuum Solvent Model

| compd | gas-phase energy (a.u.) | solvation-free energy (kcal/mol) | | log P |
|-----------------|-------------------------|----------------------------------|--------|-------|
| | | 1-octanol | water | |
| 2a | –897.242 216 152 36 | –14.41 | –17.84 | 2.51 |
| 2b | –936.570 447 282 65 | –13.21 | –16.85 | 2.66 |
| 2c | –1167.748 033 014 83 | –16.90 | –18.77 | 1.34 |
| 2d | –744.738 894 207 86 | –13.55 | –14.73 | 0.86 |
| 2e | –975.915 337 149 67 | –15.65 | –16.71 | 0.77 |
| <i>cis-3a</i> | –1920.120 733 787 47 | –24.42 | –31.96 | 5.51 |
| <i>trans-3a</i> | –1920.160 542 477 92 | –21.77 | –28.98 | 5.27 |
| <i>cis-3b</i> | –1998.766 339 879 11 | –22.34 | –30.02 | 5.61 |
| <i>trans-3b</i> | –1998.766 278 883 66 | –20.55 | –28.78 | 6.02 |
| <i>cis-3c</i> | –2461.110 998 662 73 | –22.55 | –31.81 | 6.77 |
| <i>trans-3c</i> | –2461.117 045 322 92 | –22.05 | –31.27 | 6.74 |
| <i>cis-3d</i> | –1615.098 524 661 74 | –19.79 | –25.87 | 4.44 |
| <i>trans-3d</i> | –1615.099 697 833 61 | –19.85 | –24.89 | 3.68 |
| <i>cis-3e</i> | –2077.448 947 822 58 | –20.46 | –27.41 | 5.08 |
| <i>trans-3e</i> | –2077.453 512 391 60 | –19.68 | –26.66 | 5.10 |

mented⁴² in the literature. This level was, therefore, used for the optimization of the geometries of ligands **2a–e** in the gas phase. In the structures of the isolated ligands, the most interesting result of the geometry optimization is the position of the proton in the N···H···O bridge. Although enol forms were used as the initial structures, as indicated in Table 4, the optimized structures show that the proton is close to the nitrogen atom in the optimized structures, indicating that the keto forms are more stable even in the gas phase in all cases. The effect is most pronounced in compound **2a** and increases with the polarity of the solvent (data not shown), e.g., the N–H bond becomes shorter and the O–H bond becomes longer.

In calculations incorporating solvent effects, we followed a recent report⁴³ indicating that solvation effects can be reliably obtained by the Poisson–Boltzmann (PB) method at the B3LYP/LACVP** theory level. log P values, reported in Table 5, were obtained using this approach from the free energies of solvation in water and 1-octanol. For the example of **2a**, we tested the influence of the reoptimization of the geometry within the solvent model. It was found that the solvation-free energy differences do not change significantly; the log P values at the B3LYP/LACVP** and B3LYP/LACVP**//mPW1PW91/LanL2DZ levels differ only by 0.07. Because the partial atomic charges are also practically unperturbed by the theory level at which the geometries were obtained, we used the latter level in all subsequent calculations.

Three different schemes for obtaining partial atomic charges were compared on the example of compound **2a**.

(42) Wysokiński, R.; Michalska, D. *J. Comput. Chem.* **2001**, *22*, 901–12.

(43) Lau, J. K.-C.; Deubel, D. V. *J. Chem. Theory Comput.* **2006**, *2*, 103–106.

Table 6. Partial Atomic Charges (δ) Calculated for Compound **2a** at the B3LYP/LACVP**//MPW1PW91/LanL2DZ Level

| population scheme | δ N | δ H | δ O |
|-------------------|------------|------------|------------|
| gas phase | | | |
| Mulliken | –0.41 | 0.27 | –0.45 |
| ESP | –0.59 | 0.39 | –0.56 |
| NBO | 0.69 | 0.44 | –0.64 |
| 1-octanol | | | |
| Mulliken | –0.38 | 0.29 | –0.49 |
| ESP | –0.57 | 0.41 | –0.60 |
| NBO | –0.66 | 0.44 | –0.68 |
| water | | | |
| Mulliken | –0.38 | 0.29 | –0.49 |
| ESP | –0.57 | 0.42 | –0.61 |
| NBO | –0.65 | 0.45 | –0.68 |

Table 7. Basic Geometrical Features and ESP Partial Atomic Charges on Palladium at the B3LYP/LACVP**//MPW1PW91/LanL2DZ Level

| compd | N–Pd (Å) | Pd–O (Å) | N···Pd···O (deg) | δ Pd |
|-----------------|----------|----------|------------------|-------------|
| <i>cis-3a</i> | 1.978 | 2.028 | 88.8 | 0.62 |
| <i>trans-3a</i> | 1.988 | 2.006 | 89.6 | 0.67 |
| <i>cis-3b</i> | 2.021 | 2.020 | 87.7 | 0.60 |
| <i>trans-3b</i> | 2.025 | 2.021 | 88.2 | 0.58 |
| <i>cis-3c</i> | 2.037 | 2.027 | 85.4 | 0.70 |
| <i>trans-3c</i> | 2.019 | 2.029 | 87.5 | 0.65 |
| <i>cis-3d</i> | 2.022 | 2.020 | 87.5 | 0.62 |
| <i>trans-3d</i> | 2.035 | 2.024 | 87.6 | 0.59 |
| <i>cis-3e</i> | 2.036 | 2.023 | 87.4 | 0.69 |
| <i>trans-3e</i> | 2.033 | 2.022 | 88.0 | 0.63 |

Table 6 summarizes the partial atomic charges on the nitrogen, oxygen, and hydrogen atoms obtained from Mulliken, NBO, and electrostatic fitting (ESP) analyses. As can be seen, the partial atomic charges depend significantly on the population analysis scheme. Charges obtained from the electrostatic potential fitting seem to be best balanced, and we therefore used these values in the analysis of charges on the palladium atom in its complexes.

For the ligands complexed with palladium, the optimized geometries around the palladium atom are quite similar for all of the studied compounds with the exception of **3a**, which shows significantly shorter N–Pd bonds in both conformations (see Table 7) and a slightly shorter Pd–O bond in the case of the trans isomer, resulting in slightly larger N···Pd···O angles.

Comparison of the calculated geometry of the *cis-3a* isomer with the structure obtained from X-ray diffraction indicates a very good agreement between the experimental data and the computational results. The main difference, as shown in Figure 3, lies in the torsional angle of the auxiliary

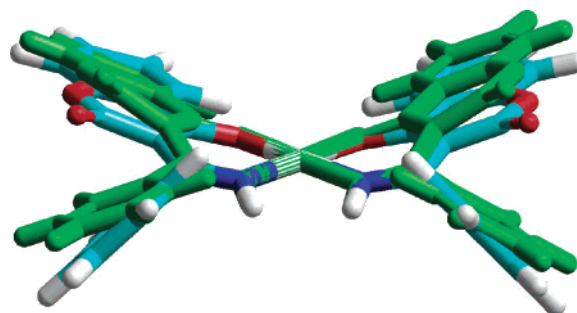
**Figure 3.** Superposition of the structures of *cis-3a* obtained from DFT calculations and X-ray diffraction.

Table 8. Relative Cis–Trans Stability^a

| compd | gas phase | 1-octanol | water |
|-----------|-----------|-----------|-------|
| 3a | 25.0 | 22.4 | 22.0 |
| 3b | 0.0 | −1.8 | −1.3 |
| 3c | 3.8 | 3.3 | 3.3 |
| 3d | 0.7 | 0.8 | −0.2 |
| 3e | 2.9 | 2.1 | 2.1 |

^a Positive means that the trans isomer is more stable.

Table 9. Cytotoxic Activities (IC₅₀, μM) of Compounds **2a–e** and **3a–e**^a

| compd | HL-60 | NALM-6 |
|-------------|--------------|--------------|
| 2a | >1000 | 784.0 ± 69.2 |
| 3a | 4.5 ± 0.6 | 2.4 ± 0.4 |
| 2b | 387.9 ± 48.4 | 486.6 ± 62.3 |
| 3b | 539.5 ± 16.6 | 548.6 ± 44.9 |
| 2c | 47.2 ± 0.41 | 45.4 ± 0.98 |
| 3c | 54.2 ± 4.30 | 51.7 ± 2.40 |
| 2d | 408.0 ± 34.0 | 276.0 ± 64.0 |
| 3d | 602.5 ± 44.3 | 84.5 ± 14.3 |
| 2e | 801.0 ± 4.7 | 83.0 ± 13.3 |
| 3e | 192.4 ± 45.8 | 209.9 ± 48.7 |
| carboplatin | 4.3 ± 1.3 | 0.7 ± 0.2 |

^a Data are expressed as mean ± SD (*n* = 4).¹⁹

rings, which is not surprising given that crystal packing can induce conformational features that are not present in the gas phase.

For the example of the *cis*-**3a** structure, we also tested (data not shown) the performance of semiempirical methods because they were reported to work very well for similar cobalt complexes.⁴⁴ Whereas the results obtained with PM3-d and PM5 were unsatisfactory, the PM6 method proved very good. The calculated geometry of the metal center is practically the same as that obtained from the DFT calculations. This observation indicates that the PM6 parametrization alone or as a part of QM/MM schemes might prove very useful in future studies of palladium-containing complexes within biological systems.

An interesting observation arises from a comparison of the relative stabilities of the *cis* and *trans* complexes. Values listed in Table 8 correlate very well with the biological activities of the *cis* compounds listed in Table 9. The significantly lower relative stability of *cis*-**3a** correlates very well with its highest cytotoxic activity. This might be the result of the highest destabilization of the *cis* isomer (compared to the *trans* isomer) among all complexes studied, making it more reactive. We were unable to find a transition state corresponding to the torsional rotation that would result in *trans*–*cis* isomerization. Because of the steric effects, it seems more likely that such isomerization proceeds by a dissociative mechanism. Obviously, more data are needed; however, should these initial observations be substantiated, it would suggest that calculations can provide a very useful tool for predicting the biological activity of such complexes.

Cytotoxicity. The cytotoxicity of compounds **2a–c** and **3a–e** was evaluated on the two human leukemia cell lines HL-60 and NALM-6. Carboplatin was used as a reference compound. Cytotoxic activity was determined over a broad

concentration range (from 10^{−7} to 10^{−3}M). The activity is expressed as the concentration required to reduce the cell survival fraction to 50% after 48 h of exposure to the compounds (IC₅₀). The results are presented in Table 9.

Discussion. For many years, only *cis* isomers were used in chemotherapy, and *trans* isomers were believed to be inactive. In the past decade, many examples of *trans*-oriented complexes that exhibit antitumor activity have been synthesized.^{45–47} These complexes exhibit strong antitumor activity, although the mechanism of their action differs from that of their *cis* counterparts. We synthesized a series of ligands with substituents such as H, CH₃, or CH₂Ph at the nitrogen or benzylidene or ethylidene at the C3 atom. We observed that the formation of the *trans* or *cis* isomer is governed by the size of the substituent at the nitrogen atom, i.e., bulky groups lead to the *trans* isomer, whereas compounds with unsubstituted nitrogen atoms exist as the *cis* isomer.

We observed that, for ligands **2a–c**, the cytotoxic effect increases with increasing size of the substituent at the nitrogen atom, as the IC₅₀ values were 784.0, 486.6, and 45.4, respectively, for the NALM-6 cell line. For compounds **2d,e**, carrying the ethylidene group on the C3 atom of coumarin, the cytotoxic effect increases in the same way. The synthesized complexes were more toxic toward the NALM-6 leukemia cell lines than toward HL-60. The palladium *cis* complex **3a** exhibited the highest cytotoxicity toward the HL-60 and NALM-6 cells, with IC₅₀ coefficients of 4.5 and 2.4 μM, respectively, i.e., close to those for carboplatin. As reported in Table 9, palladium complexes **3b–e** have somewhat lower cytotoxic activities than carboplatin. In contrast to the *cis* complexes, the *trans* counterparts show remarkable cytotoxicity to both cell lines. It is interesting to note that ligand **2a** exhibits a very low cytotoxic activity. Initial antitumor studies show that the cytotoxic activity of the synthesized palladium(II) complexes depends significantly on the structure of the substituents at the nitrogen atom.

Lipophilicity is one of the most important factor for the design of new drugs.⁴⁸ The mechanisms of resistance to cisplatin have been identified as decreased drug accumulation, increased cytoplasmic detoxification, and increased DNA repair.⁴⁹ Structure–cytotoxicity relationship studies have also revealed that, for many compounds, increased lipophilicity is often accompanied by increased cytotoxicity.⁵⁰ In our investigations, we did not observe any correlation between cytotoxicity and lipophilicity. Compounds **2a–c** exhibit a higher lipophilicity than compounds **2d,e**. Calculations indicate that there is correlation between the relative stabilities of the *cis* and *trans* complexes and the cytotoxicity.

(45) Kasparikova, J.; Marini, V.; Najareh, Y.; Gibson, D.; Brabec, V. *Biochemistry* **2003**, *42*, 6321–6332.

(46) Natile, G.; Coluccia, M. *Coord. Chem. Rev.* **2001**, *216–217*, 383–410.

(47) Radulovic, S.; Tesic, Z.; Manic, S. *Curr. Med. Chem.* **2002**, *9*, 1611–1618.

(48) Hall, M. D.; Hambley, T. W. *Coord. Chem. Rev.* **2002**, *232*, 49–67.

(49) Welland, L. R. *Eur. J. Cancer* **1994**, *30A*, 725.

(50) Kupchan, S. M.; Eakin, M. A.; Thomas, A. M. *J. Med. Chem.* **1971**, *14*, 1147–1152.

(44) Kwiecień, R.; Rostkowski, M.; Dybała-Defratyka, A.; Paneth, P. *J. Inorg. Biochem.* **2004**, *98*, 1078–1086.

On the basis of the observation that Pd(II) complexes exchange their leaving groups 105 times more easily than their Pt(II) analogues,⁵¹ the low antitumor activity of Pd compounds has been attributed to the rapid hydrolysis of the leaving groups, which dissociate readily in solution leading to very reactive species that are unable to reach their pharmacological targets.^{52,53} We investigated the stability of the synthesized compounds. The significantly lower thermodynamic stability of *cis*-**3a** compared to *trans*-**3c** corresponds to its highest cytotoxic activity. Obviously, more data are needed to make sure that the correlation is not coincidental. However, should it prove real, it would render calculations a very strong predictive tool of biological activity.

Conclusions. In this article, we have shown a simple and convenient route for the synthesis of *cis*- and *trans*-oriented Pd complexes. The newly synthesized ligands **2a–e** create neutral complexes of the general ML₂ type. We observed that, depending on the size of the substituent on the nitrogen atom, the *trans* or *cis* complexes are formed. The structures of complexes **3a** and **3c** were confirmed using X-ray diffraction. Both complexes *cis*-**3a** and *trans*-**3c** exhibit

square-planar geometries around the Pd(II) atom. The results clearly indicate coordination via N and O heteroatoms.

The present study demonstrates that the Pd(II) complexes of the coumarin ligands **2a–e** exhibit potential cytotoxic activity toward HL-60 and NALM-6 leukemia cells, with cytotoxicity coefficients IC₅₀ similar to those of carboplatin. Compound **3a** seems to be promising as an anticancer agent because of its high cytotoxic activity. Additionally, its ligand **2a** is practically inactive. The computational analysis, carried out at the PB/B3LYP/LACVP**//mPW1PW91/LanL2DZ theory level, indicates that the *cis* complexes are thermodynamically less stable than their *trans* counterparts and that this difference seems to correlate well with the biological activity.

Acknowledgment. Financial support from the Medical University of Łódź (Grant 502-13-287 to E.B.), Technical University of Łódź, and University of Lodz (Grants 505/696 and 3T09A_138_26KBN to M.M.) and access to the supercomputing facilities at ICM Warsaw and PCSS Poznan are gratefully acknowledged. The authors thank Prof. Werner Massa from University of Marburg for skilful experimental assistance.

Supporting Information Available: Crystal data and positive-ion ESMS spectrum of **3a**. This material is available free of charge via the Internet at <http://pubs.acs.org>.

IC0605569

- (51) Shourky, A.; Rau, T.; Shourky, M.; van Eldik, R. *J. Chem. Soc., Dalton Trans.* **1998**, 3105–3112.
(52) Macquet, J. P.; Butons, J. L. *J. Natl. Cancer. Inst.* **1983**, *70*, 899–905
(53) Zhao, G.; Sun, H.; Lin, H.; Zhu, S.; Su, X.; Chen, Y. *J. Inorg. Biochem.* **1998**, *72*, 173–177.